Borneo Engineering: Jurnal Teknik Sipil
Vol. 10 No. 1. April 2026, pp. 54-64

ISSN 2685-7553
e-**ISSN 2581-1134**

Research Article

The Effect of Relative Density of Geosynthetic Encased Stone Columns on the Bearing Capacity and Consolidation of Soft Soil

Julita Hayati[1*], Johanes Simamora[1], and Arif Rahman Hakim Sitepu[1]

[1]Civil Engineering Study Program, Faculty of Infrastructure and Regional Technology, Institut Teknologi Sumatra, Lampung, Indonesia.

[*]Corresponding author: julita.hayati@si.itera.ac.id
DOI. 10.35334/be.v10i1.574

Article history:
Received: Des 16, 2025
Revised: Apr 4, 2026
Accepted: Apr 11, 2026

Keywords:
bearing capacity,
finite element method,
geosynthetic-encased stone column,
settlement,
soil improvement.

Abstract

The behavior of soft soil presents a challenge when constructing roads on it. The low bearing capacity is the primary issue, accompanied by significant settlement due to the soil's high compressibility. In the Indrapura-Kisaran STA 111+505 – STA 112+300 Toll Road Construction project, there is a 10,45 m-thick soft soil with undrained shear strength = 6 kN/m² and a bearing capacity of 30,84 kN/m², so soil reinforcement is needed. The reinforcement method used is Geosynthetic Encased Stone Columns (GESC). The density of the GESC material used in this method should be evaluated to assess GESC's effectiveness in reducing settlement and increasing soil bearing capacity. The analysis process in this study involves assessing reinforcement using GESC with both empirical and numerical methods. This study uses relative densities of the column material at 25%, 50%, 75%, and 100%. After reinforcement, the soil's bearing capacity increased by 280,37%- 361,71%. Additionally, GESC reinforcement reduced settlement by up to 64,96% using the analytical method and 41,6% using the numerical method, and reduced consolidation time by 93,38%-94,52%. The reduction in relative soil density causes settlement to increase by ±7,2% because the friction angle of the column decreases.

Introduction

Sumatra Island is Indonesia's second-largest island, endowed with a wealth of natural resources that play a vital role in the country's economy. To achieve this, the government is building the Trans-Sumatra Toll Road to connect Aceh and Lampung, thereby supporting the local economy through trade, services, and markets and stimulating regional economic growth. One section of the Trans-Sumatra toll road is the Indrapura-Kisaran Toll Road, planned to connect Indrapura, Limapuluh, and Kisaran, spanning 47,75 km.

During planning for the Indrapura-Kisaran Toll Road construction, a soil investigation was conducted, which found that the road section contained soft soil. Soft soil is a problem because it has low bearing capacity, a relatively long consolidation time, and causes significant long-term settlement due to its high compressibility. Therefore, soil improvement is necessary to overcome this problem. Several soil improvement methods, such as adding sand, can enhance the soil's physical properties. Saputra et al. (2025) studied the addition of sand to soft soil, which effectively increased the maximum dry density value. However, this method does not significantly and quickly improve the physical and mechanical properties, so the use of soil reinforcement is considered more significant and faster. One soil reinforcement option is a stone column.

According to Han (2015) stone columns can be used as reinforcement because they increase bearing capacity, accelerate consolidation, have relatively low material costs, and reduce settlement. However, stone columns have a weakness: in very soft soil conditions with undrained shear strength (Su) values less than 15 kPa, their use becomes ineffective due to excessive lateral deformation, thereby reducing their ability to increase bearing capacity and reduce settlement. To overcome this weakness, geosynthetics can be added vertically or as a wrap to reduce the effects of lateral deformation. Chen et al. (2015) stated that the addition of geosynthetics to stone columns can increase the safety factor against shear failure by increasing the stiffness and load capacity of the column.

In stone columns, column density reduces settlement by increasing stiffness, as shown by Bergado & Lam (1987). The study found that, in stone columns, bearing capacity increased with increasing material density. Herle I., Wehr J (2015). Conducted field tests that showed that dense columns provide almost twice the bearing capacity of loose columns. However, with stone columns, achieving high density and precise field measurements is difficult. Therefore, geosynthetics are used to encapsulate stone columns, providing much greater stiffness. Murugesan & Rajagopal (2006). Conducted a series of tests on single columns and groups of conventional stone columns, as well as geosynthetic-encased stone columns (GESC). The test results indicated an increase in bearing capacity with the use of GESC. In a study by Alexiew et al. (2015) the installation of GEC during the construction of the HSL Paris-Amsterdam in Westrik resulted in a settlement of only about 10 cm and a very fast consolidation time. Hosseinpour, Almeida and Riccio (2016) stated that installing GECs on soft soils can accelerate the dissipation of excess pore water pressure, based on monitoring results during loading. Hayati et al. (2025) conducted a study showing that installing GESCs on soft soils can reduce settlement by up to 86% and increase soil bearing capacity by up to 84%, with these effects influenced by the tensile strength of the geosynthetics, installation distance, and installation pattern. Miranda et al. (2015) reported a 10% reduction in settlement as the relative density of gravel increased from 30% to 100%.

However, little research has examined the effect of changes in the density of geosynthetic-encased stone columns. Therefore, this study will examine subgrade reinforcement using geosynthetic-encased stone columns by analyzing the effect of variations in material density on bearing capacity, subgrade settlement, and consolidation time.

Research Methods

This quantitative study analyzed soil conditions at the Indrapura-Kisaran Toll Road Development project site, STA 111+505–STA 112+300, in Batubara Regency, North Sumatra Province, using empirical and numerical (finite-element) analyses. Based on field soil investigation data, a soft sandy silt layer (NSPT = 1) is found at a depth of 1–11,45 m. A 6,37 m embankment will be installed to achieve the final road elevation.

In the finite element analysis, soil investigation data are required to generate design soil parameters. Subgrade parameters (Table 2) are derived from laboratory test data (Table 1) and NSPT testing. Data on soil physical properties and consolidation are used in the empirical and numerical analyses. In contrast, the soil shear strength, permeability, modulus of elasticity, and Poisson's ratio are derived from empirical correlations of NSPT data. In the numerical analysis, fine-grained soil is modeled as Undrained-Soft Soil and coarse-grained soil as Drained-Mohr Column. Soft-soil parameters: compression index (λ^*) and swelling index (k^*) are calculated according to the Material Model in the PLAXIS 2025 Manual. The embankment material is selected embankment soil with a cohesion shear strength parameter of 13,10 kPa.

In finite element modeling, the geometric boundary conditions at the ground surface (BoundaryYmax) are free in all directions, and at the base (BoundaryYmin) are fixed in all directions. Meanwhile, the x-direction (BoundaryXmax and BoundaryXmin) is fixed in the x-direction and free in the y-direction. The construction stages in the modeling consist of the initial phase, the GESC installation phase, the backfill phase, and the consolidation phase. The backfill phase is carried out in stages (4 stages) for conditions without GESC, taking into account the gained strength.

Table 1. Laboratory Test Data

Parameters	Symbol	Unit	Value	
Depth		m	2,3 - 3	6,3 - 7
Specific Gravity	Gs		2,56	2,49
Bulk unit weight	γ_{sat}	kN/m^3	16,2	17,97
Bulk density	γ	kN/m^3	10,68	13,63
water content	w	%	51,7	31,91
Liquid limit	LL	%	59	29
Plastic limit	PL	%	34	24
Plasticity index	LL	%	25	4
Void ratio	e		1,35	0,79
Porosity	n	%	57	44
Degree of saturation	S	%	98	100
Sensitivity	St		1,5	-
Compression index	Cc		0,45	0,38
Recompression index	Cr		0,028	0,04
Preconsolidation pressure	Pc'	kPa	434,8	**680,3**

Table 2. Basic Soil Parameters

Parameters	Unit	Value			
Depth	m	0-1	1-6	6 - 11,45	11,45 - 30,45
Condition		Drained	Undrained	Undrained	Drained
Model		Mohr Coulomb	Soft Soil	Soft Soil	Mohr Coulomb
Soil type		Silty Sand	Sandy Silt	Sandy Silt	Silty Sand
Void ratio	e	0,746	1,35	0,79	0,378
Saturated unit weight	kN/m^3	18	16,2	17,97	21
Bulk density	kN/m^3	15	10,68	13,63	19
Undrained cohesion	kPa	-	6	6	-
Effective cohesion	kPa	-	0,6	0,6	-
Friction angle	°	33	17	17	39,93970503
Poisson's ratio	υ	0,25	0,45	0,35	0,25
Modulus of elasticity	kN/m^2	6505	2100	2100	20000
Permeability	m/days	8,64 x 10^{-2}	1,77 x 10^{-4}	1,43 x 10^{-4}	864 x 10^{-1}
Compression index	λ*	-	8,33 x 10^{-2}	9,23 x 10^{-2}	-
Swelling index	k*	-	10,4 x 10^{-2}	1,94 x 10^{-2}	-
Preconsolidation pressure	kPa	-	434,8	680,3	-

This study will analyze the bearing capacity, subgrade settlement, and consolidation time of a reinforced subgrade with geosynthetic-encased stone columns. The variations used are the relative density percentages of the stone column material, at 25%, 50%, 75%, and 100%. According to Federal Highway Administration regulations, the recommended alternative material is classified as poorly graded gravel (GP). Therefore, using Figure 1, the friction angle for each variation used can be obtained.

Furthermore, for the stone column parameter values, empirical correlations and relative density variation approaches to the friction angle, NSPT value, and dry unit weight are used, as referenced in Bowles (1997). The stone column parameters are shown in Table 3.

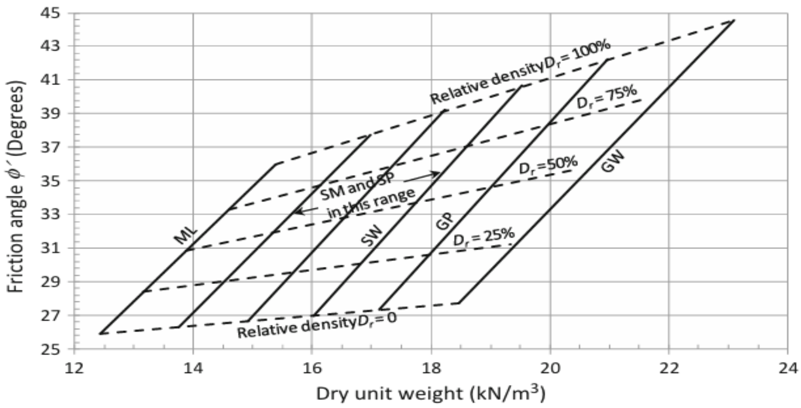

Figure 1. Friction Angle of Granular Soil (Ameratunga et al., 2016)

Table 3. Stone Column Parameters

Parameters	Unit	SC 1	SC 2	SC 3	SC 4
		Value			
Relative density	%	25	50	75	100
Friction angle	°	30,6	34,6	38,6	42,2
Model		Mohr Coulomb	Mohr Coulomb	Mohr Coulomb	Mohr Coulomb
Void ratio		0,455	0,37	0,309	0,247
Specific Gravity		2,67	2,67	2,67	2,67
Saturated unit weight	kN/m³	21,068	21,694	22,318	22,945
Bulk density	kN/m³	18	19	20	21
Permeability	m/s	10	10	10	10
Dilatancy angle	°	0,6	4,6	8,6	12,2
Poisson ration		0,3	0,3	0,3	0,3
Modulus of elasticity	kN/m²	17184	30880	50080	67360
N		8	28	44	59

When designing geosynthetic-encased stone columns, several considerations are required, including the installation pattern, column diameter, and spacing. This study used a triangular installation pattern, an installation spacing of 1,5 m, and a column diameter of 0,9 m. These values were then used to calculate the equivalent diameter and the area replacement ratio, as given by equations 1 and 2.

$$D_e = 1{,}13 \times S \tag{1}$$

$$a_s = \frac{A_c}{A_c} = C\left(\frac{d_c}{s}\right)^2 \tag{2}$$

In the formula, De is the equivalent diameter for the triangular pattern, S is the installation distance (m), Ac is the column cross-sectional area (m²), and Ae is the area of influence around the column (m²). Meanwhile, dc represents the column diameter (m), s indicates the distance between the column centers, and C is a constant (triangular pattern = = $\pi/2\sqrt{3}$ or 0,907, and rectangular pattern = $\pi/4$ or 0,785).

When the embankment load acts on a geosynthetic-encased stone column and the surrounding soil, vertical stresses (overburden stresses) are transmitted to the column and soil. Due to the vertical stresses in the soil and column, as well as the additional stresses from the embankment, lateral or radial stresses are generated. Equations 3 and 4 are used to estimate the magnitude of these stresses.

$$\sigma_{r,c} = \Delta\sigma_c \times K_{a,c} + \sigma'_{z0,c} \times K_{a,c} \tag{3}$$

$$\sigma_{r,s} = \Delta\sigma_s \times K_{0,s} + \sigma'_{z0,s} \times K_{0,s} \tag{4}$$

In this equation, $\sigma'_{z0,c}$ represents the effective overburden stress on the column (kN/m²), while $\sigma'_{z0,s}$ represents the effective overburden stress on the soil (kN/m²). Furthermore, $\sigma_{r,c}$ represents the lateral stress acting on the column (kN/m^2), while $\sigma_{r,s}$ represents the lateral stress acting on the surrounding soil (kN/m^2). The notation $\Delta\sigma_c$ is used to denote the increase in vertical stress on the column (kN/m^2), while $\Delta\sigma_s$ indicates the increase in vertical stress on the surrounding soil (kN/m^2). $K_{a,c}$ is the active earth pressure coefficient on the column, while $K_{0,s}$ is the lateral stress coefficient of the soil in at-rest conditions on the surrounding soil.

Because lateral stress can cause lateral deformation, a geosynthetic wrap is used as lateral resistance. The geosynthetic layer is assumed to be a linear elastic material with a stiffness modulus (J). Gouw (2015) provides the following equation for calculating the stiffness modulus of a geosynthetic.

$$T_{all} = \frac{T}{RF_{CR} \times RF_{ID} \times RF_{CBD}} \tag{5}$$

$$J = \frac{T_{all}}{\varepsilon} \tag{6}$$

In this equation, J denotes the modulus of stiffness of the geosynthetic, expressed in kN/m, while ε represents the elongation of the material under tensile loading. The term T_{all} refers to the allowable tensile strength of the geosynthetic (kN/m), whereas T indicates its ultimate tensile strength (kN/m). Furthermore, the design tensile capacity is adjusted by several reduction factors, including RF_{CR} for creep effects, RF_{ID} for damage or strength loss during installation, and RFCBD for degradation due to chemical and biological agents.

Table 4. Geosynthetic Tensile Strength Reduction Factor

Application	RF_{CR}	RF_{ID}	RF_{CBD}
Separation	1,5–2,5	1,1– 2,5	1 – 1,5
Cushioning	1,2 – 1,5	1,1 - 2	1 - 2
Unpaved roads	1,5 – 2,5	1,1 - 2	1 – 1,5
Walls	2 - 4	1,1 - 2	1 – 1,5
Embankments	2 – 3,5	1,1 - 2	1 – 1,5
Bearing and Foundations	2 - 4	1,1 - 2	1 – 1,5
Slope stabilization	2 - 3	1,1– 1,5	1 – 1,5
Pavement overlays	1 - 2	1,1– 1,5	1 – 1,5
Railroads	1 – 1,5	1,5 - 3	1,5 - 2
Flexible forms	1,5 - 3	1,1– 1,5	1 – 1,5
Silt fences	1,5 – 2,5	1,1– 1,5	1 – 1,5

Source: Ameratunga et al. (2016)

Alexiew & Thomson (2013) assume that the geosynthetic radius is the same as the casing radius of the column (rg = rc), so that the strain on the geosynthetic is the same as the strain on the GESC column (Δrg = Δrc). The lateral stress on the geosynthetic covering the GESC column is calculated using the following equations 7 and 8.

The magnitude of the tensile strength reduction factor for geosynthetics, classified by use, is presented in Table 3 below. In this study, the geosynthetic used as a stone column wrapper is a woven type with a tensile strength of 400 kN/m and a maximum elongation limit value of 5% (Table 5).

Table 5. Geosynthetic Parameter Data

Data	Unit	Value
Tensile strength	kN/m	400
Elongation	ε	0,05
Creep factor	RFcr	3
Installation damage reduction factor	RFid	1,1
hemical and biological degradation reduction factor	RFcbd	1,1
Ultimate tensile strength	kN/m	110,192
Tensile stiffness	J(kN/m)	2230,856

Source: Ameratunga et al. (2016)

$$\sigma_{r,g} = J\frac{\Delta r_c - (r_g - r_c)}{{r_g}^2} \tag{7}$$

$$\Delta r_c = \frac{\sigma_{r,c} - \sigma_{r,s} + \frac{(r_g - r_g)}{{r_g}^2}}{\frac{a_s E^*}{(1-a_s)r_c} + \frac{J}{{r_g}^2}} \tag{8}$$

In the equation, $\sigma_{r,g}$ represents the lateral stress on the geosynthetic wrap (kN/m²), while r_g indicates the radius of the geosynthetic in units (m). Furthermore, r_c denotes the radius of the GESC column (m), and me denotes the area replacement ratio, which describes the proportion of the column area to the reinforced area. Meanwhile, E^* is the equivalent modulus due to the influence of GESC (kN/m²).

During loading, vertical deformation occurs in the GESC column, followed by horizontal bulging at its top. This bulging area, also referred to as the column bulging area, causes the geosynthetic wrapping of the GESC column material to stretch, producing hoop tensile stresses that increase the column's stress. considered the increased restraint provided by the geosynthetic wrapping on the ultimate bearing capacity of a single column due to the possibility of bulging failure with a bulging length of four times the column diameter. The ultimate bearing capacity of a single column was calculated using the following equations 9 and 10

$$q_{ult,c} = (\sigma_{r0} + 4c_u + \sigma_{r,g})K_{p,c} \tag{9}$$

$$\sigma_{r0} = \sigma'_{z0,s4D} \times K_{0,s} + \Delta\sigma_s \times K_{0,s} \tag{10}$$

In this equation, $q_{ult,c}$ denotes the ultimate bearing capacity of a single column, expressed in kN/m², which represents the maximum load that the column can sustain before failure. The parameter c_u denotes the undrained shear strength of the surrounding soil (kN/m²), representing the soft soil's resistance to shear deformation under undrained conditions. Furthermore, $K_{p,c}$ is the passive earth pressure coefficient of the column, which reflects the contribution of lateral confinement to the column's load-bearing performance. The term σ_{r0} represents the lateral soil stress induced by the overburden stress at the mid-height bulging zone of the column (kN/m²), while $\sigma'_{z0,s4D}$ denotes the overburden stress of the surrounding soil at the bulging zone of the column (kN/m²).

Since the granular columns and the surrounding soil attain strength at similar strain rates (composite), the ultimate bearing capacity of a composite foundation reinforced with granular columns can be calculated using equation 11

$$q_{ult} = q_{ult,c} \times a_s + q_{ult,s} \times (1 - a_s) \tag{11}$$

where, q_{ult} is the bearing capacity of the composite column (kN/m^2), and $q_{ult,s}$ is the bearing capacity of the soil around the column (kN/m^2)

The bearing capacity of the soil around the column ($q_{ult,s}$) is estimated at ($5 \times c_u$). To estimate the settlement that occurs in a geosynthetic encased stone column, Raithel & Kempfert (2000) proposed equations 12 and 13, which are based on the unit cell concept.

$$S_{sl} = \left[\frac{\Delta\sigma_s}{D_s} - \frac{2}{E^*}\left(\frac{v_s}{1-v_s}\right)\Delta\sigma_r\right] \tag{12}$$

$$S_{cl} = \left[1 - \frac{r_c^2}{(r_c + \Delta r_c)^2}\right] \tag{13}$$

where D_s is the modulus of restraint of the soil (kN/m^2), and $\Delta\sigma_r$ is the difference in lateral stress between the column and the soil and the geosynthetic (kN/m^2).

Numerical analysis was conducted to obtain comparative results against the empirical analysis. Numerical analysis allows simulation of various conditions without the need for physical experiments, but the results are highly dependent on the assumptions and parameters used in the model. In this study, plane strain modeling was used because it was deemed more suitable for the case study. Modeling with plane strain has a different visual perception than the real-world situation. Therefore, to analyze GESC using plane strain modeling, it is necessary to convert from axisymmetric by reducing the diameter of the GESC.

Almeida et al. (2015) stated that granular columns are simulated with equivalent plane-strain walls, and that half the diameter of the column modeled in plane strain can be determined using equations 14, 15, and 16.

$$b_c = B\frac{r_c^2}{R^2} \tag{14}$$

$$B = \frac{R}{1{,}13} \tag{15}$$

$$R = \frac{D_e}{2} \tag{16}$$

Where, b_c is the radius of the column modeled with plane strain (m), r_c is the actual radius of the column (m), B is half of the area affected by the plane strain (m), and R is the radius of the unit cell (m).

In plane-strain modeling, the restraint provided by the geosynthetic wrap on the GESC can be modeled by equivalentizing the shear angle of the column granular material. The magnitude of the equivalent granular column shear angle value can be calculated using the following equation (Hosseinpour et al., 2017).

$$\sin\phi'_{sub} = \frac{\dfrac{1+\sin\phi'_c}{1-\sin\phi'_c} + \dfrac{\sigma_{r,g}}{\sigma_{r,c}} - 1}{\dfrac{1+\sin\phi'_c}{1-\sin\phi'_c} - \dfrac{\sigma_{r,g}}{\sigma_{r,c}} + 1} \tag{17}$$

where, ϕ'_{sub} is the equivalent shear angle of the column granular material (°), ϕ'_c is the shear angle of the GESC column granular material (°), $\sigma_{r,c}$is the lateral stress on the column (kN/m^2) and $\sigma_{r,g}$ is the lateral stress of the geosynthetic wrap (kN/m^2).

Table 6. Summary of ϕ'_{sub} Values

Dr (%)	**ϕ'_c (°)**	**Sin ϕ'_{sub}**	**ϕ'_{sub} (°)**
25	30,6	0,624	38,619
50	34,6	0,668	41,963
75	38,6	0,710	45,246
100	42,5	0,747	48,392

The equivalent friction angle values and dimensional data of geosynthetic-encased stone column modeling are shown in Table 6. The dimensional data of GESC are shown in Table 7.

Table 7. GESC Dimensional Data in Plane Strain Modeling

Data	**Unit**	**Value**
Diameter	m	0,9
Radius	m	0,45
Spacing	m	1,5
Equivalent	m	1,575
Equivalent radius	m	0,7875
½ equivalent width of the plane strain influence area	m	0,75
½ width of the plane strain column	m	0,244897959
Plane strain diameter	m	0,490

Results and Discussion

Analysis of the Effect of Geosynthetic Encased Stone Columns on the Bearing Capacity of Subgrade

In this case study, the original soil bearing capacity was 30,84 kN/m². Calculations revealed that increasing the relative density (Dr) of the encased stone column (GESC) material increased the soil bearing capacity, with the increase in bearing capacity rising as stone column density increased. The effect of increasing stone column density on bearing capacity is shown in Figure 2.

The bearing capacity of GESC-reinforced soil is influenced by the bearing capacity of the column and the surrounding soil (equation 11). Based on equation 9, the column's ultimate bearing capacity is highly dependent on the friction angle of the stone column material due to the influence of lateral earth stress and the passive earth pressure coefficient. The higher the friction angle of the column material, the higher the passive earth pressure coefficient, thereby increasing the soil bearing capacity. The friction angle of the column material has a linear relationship with the relative density (Dr). According to a study Elwakeel & Elsherbini (2025) increasing the internal friction angle of column materials directly increases resistance to lateral deformation (bulging) and optimizes hoop forces in the geosynthetic envelope. This mechanism results in increased overall foundation bearing capacity and a more effective reduction in soft-soil settlement.

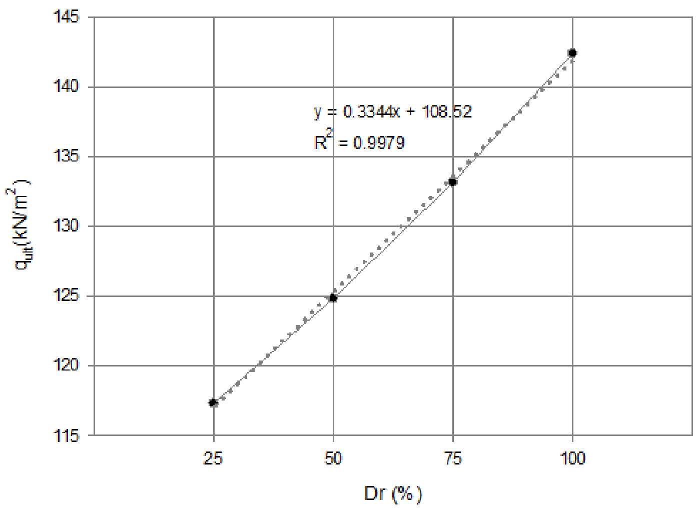

Figure 2. Graph of The Relationship Between Soil Bearing Capacity and Relative Density (Dr) of Stone Column Material

Based on Table 8, the soil bearing capacity increases after improvement using the GESC method. For GESC with a density of 25%, there is an increase in the value of the bearing capacity of 280,37%; for GESC with a density of 50%, there is an increase in the value of the bearing capacity of 304,72%; for GESC with a density of 75%, there is an increase in the value of the bearing capacity of 331,77%, for GESC with a density of 100%, there is an increase in the value of the bearing capacity of 361,71%.

Table 8. Recapitulation of Theoretical Axial Bearing Capacity

Dr (%)	ϕ'_c (°)	$\gamma_{c(unsat)}$ (kN/m³)	qult (kN/m²)	Increase qult (%)
25	30,6	21,068	117,304	280,37%
50	34,6	21,693	124,816	304,72%
75	38,6	22,319	133,157	331,77%
100	42,5	22,944	142,391	361,71%

The increase in bearing capacity due to the use of GESC can occur because, along with the increase in density, there is an increase in the passive coefficient value (Kp, c) of the column. The value of this passive coefficient column indicates how much the column resists the resulting lateral force. The value of the passive coefficient of the column is directly proportional to the value of the column's bearing capacity, so that with an increase in the value of the passive coefficient of the column, the value of the bearing capacity of the column will also increase. In addition, this is also influenced by the lateral stress formed in the column, where the increase in the density value causes a reduction in the value of the lateral stress of the column (σr, c) and soil (σr, s) which can reduce excessive deformation of the column (Δrc) so that it can increase the bearing capacity of the soil improved with GESC.

Analysis of the Effect of Geosynthetic Encased Stone Columns on Subgrade Consolidation Settlement

The relative density of the column affects soil settlement, settlement decreases as the density of the stone column material increases.

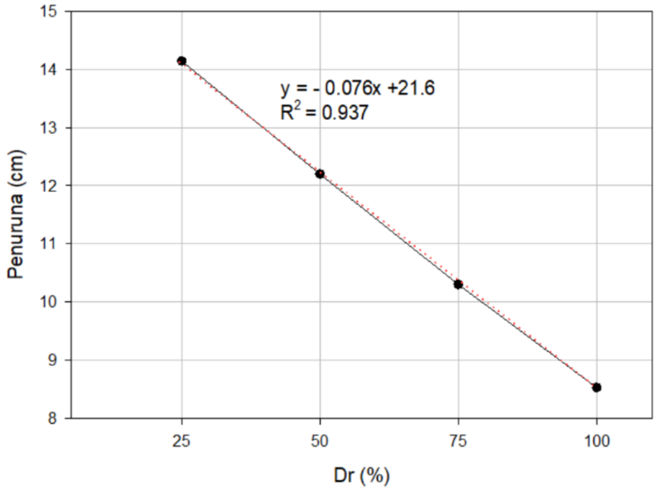

Figure 3. Graph of Land Subsidence Against Relative Density (Dr) for the Empirical Method

Figure 3 shows the relationship curve between relative density (Dr) and settlement based on empirical calculations, and Figure 4 shows the relationship curve between relative density (Dr) and settlement based on numerical calculations. Increasing relative density results in a reduction of approximately 2–3 cm. This is because settlement is influenced by material stiffness: the stiffer the material or column, the less the load affects the magnitude of settlement. Columns with higher densities exhibit greater stiffness. Relative density influences settlement, with settlement generally being lower in the case of soils with higher relative densities (Fakher & Fakhruldin, 2021).

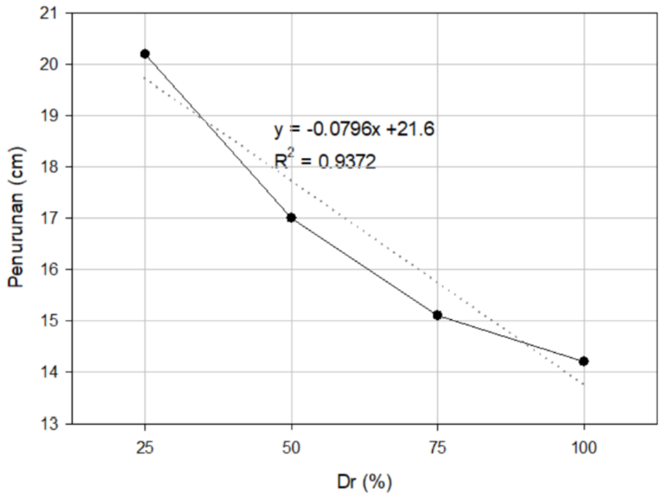

Figure 4. Graph of Land Subsidence Against Relative Density (Dr) for the Numerical Method

The results of the empirical and numerical calculations show differences. The empirical analysis used the unit cell method introduced by Raithel and Kempfert Han (2015). This method relies on several assumptions to estimate the magnitude of settlement: equal settlement at the top and bottom of the GESC; no settlement below the column tips; granular columns are assumed incompressible; and the design is based on drained conditions.

These assumptions indicate that the resulting settlement is not due to vertical deformation but rather to the redistribution of lateral stress in the surrounding soil, leading to bulging, lateral deformation, and consolidation. This rationale is also supported by the results for vertical soil stress (Δσs), column stress (Δσs), resulting lateral column stress (σr,c), and resulting deformation (Δrc).

The numerical analysis using the 2-dimensional finite element method revealed greater settlement than the empirical method. According to Almeida et al. (2013) empirical methods do not account for the development of plastic points in the soil, making them accurate only within the elastic strain range or at low loads. In contrast, numerical models can simulate the formation of plastic zones in both the column and the surrounding soft soil as the embankment load increases, thereby yielding larger settlement predictions that more closely reflect actual field conditions. In addition to the plasticity factor, empirical methods assume equal settlement between the column and the surrounding soil to simplify calculations. Furthermore, numerical methods allow the calculation of load transfer and settlement for each element separately, thereby capturing more complex nonlinear stress distributions. Because empirical methods ignore the additional plastic deformation that occurs when the soil reaches its strength limit, they tend to underestimate settlement compared to finite element modeling.

In addition, the difference in settlement results is caused by the empirical settlement calculation, where the influence of geosynthetics is also considered as a limitation, while in the numerical settlement calculation the tensile strength value of the geosynthetics is converted into an additional friction angle of the stone column material so that the effect of the geosynthetics used is not optimal and causes greater lateral deformation.

Conclusion

This study demonstrates that the use of Geosynthetic Encased Stone Columns (GESC) is highly effective in improving the characteristics of soft soil in toll road projects. The main findings indicate a significant increase in soil bearing capacity of 280,37% to 361,71%, as well as a reduction in consolidation time of up to 94,52%. The performance of GESC is strongly influenced by the relative density (RD) of the infill material; an increase in RD has been shown to increase the material's internal friction angle, thereby strengthening the interlocking effect and the column's stiffness. This is directly proportional to the reduction in lateral deformation (bulging), where a 25% decrease in relative density can increase the settlement value by ±7,2%. Technically, the numerical method (FEM) yields more accurate and realistic settlement predictions than the empirical method because it can simulate the soil's elastoplastic behavior and the formation of plastic zones. The engineering implications of this study emphasize that material density control during GESC installation in the field is crucial to ensure maximum bearing capacity and minimize long-term settlement in construction on soft soils.

Conflicts of Interest

The authors declare no conflict of interest.

References

Alexiew, D., Raithel, M., Schimmel, L., & Schröer, S. (2015). Geotextile Encased Columns (GEC) as pile-similar foundation elements: Basics, specifics, case studies. *40th Annual Conference on Deep Foundations*, 441–452.

Alexiew, D., & Thomson, G. (2013). Foundations on Geotextile Encased Granular Columns: Overview, Experience, Perspectives. *Proceedings of the International Symposium on Advances in Foundation Engineering*, 401–407. https://doi.org/10.3850/978-981-07-4623-0_115

Almeida, M. S. S., Hosseinpour, I., & Riccio, M. (2013). Performance of a geosynthetic-encased column (GEC) in soft ground: numerical and analytical studies. *Geosynthetics International*, *20*(4), 252–262. https://doi.org/10.1680/gein.13.00015

Almeida, M. S. S., Hosseinpour, I., Riccio, M., & Alexiew, D. (2015). Behavior of Geotextile-Encased Granular Columns Supporting Test Embankment on Soft Deposit. *Journal of Geotechnical and Geoenvironmental Engineering*, *141*(3). https://doi.org/10.1061/(ASCE)GT.1943-5606.0001256

Ameratunga, J., Sivakugan, N., & Das, B. M. (2016). *Developments in Geotechnical Engineering Correlations of Soil and Rock Properties in Geotechnical Engineering*. http://www.springer.com/series/13410

Bergado, D. T., & Lam, F. L. (1987). Full Scale Load Test of Granular Piles with Different Densities and Different Proportions of Gravel and Sand on Soft Bangkok Clay. *Soils and Foundations*, *27*(1), 86–93. https://doi.org/10.3208/sandf1972.27.86

Bowles, J. E. (1997). *Foundation Analysis and Design* (5th ed.). The McGraw-Hill Companies.

Chen, J.-F., Li, L.-Y., Xue, J.-F., & Feng, S.-Z. (2015). Failure mechanism of geosynthetic-encased stone columns in soft soils under embankment. *Geotextiles and Geomembranes*, *43*(5), 424–431. https://doi.org/10.1016/j.geotexmem.2015.04.016

Elwakeel, A. O., & Elsherbini, R. M. (2025). Effect of Column Material Internal Angle of Friction and the Geotextile Stiffness on the Behavior of Group of Geosynthetic-Encased Stone Column. *Indian Geotechnical Journal*, *55*(3), 1428–1442. https://doi.org/10.1007/s40098-024-01005-5

Fakher, N. A., & Fakhruldin, M. K. (2021). Experimental Study of Relative Density Effect on Bearing Capacity of Sand Reinforced with Geogrid. *Kufa Journal of Engineering*, *12*(3), 46–55. https://doi.org/10.30572/2018/kje/120304

Gouw, T. L. (2015). Importance of Elongation Factor in Determining Geosynthetics Stiffness for Finite Element Calculation. *International Conference on Landslides and Slope Stability*, B81-B8-6.

Han, J. (2015). *Principles and Practices of Ground Improvement*. John Wiley & Sons, Inc.

Hayati, J., Syuhada, S., & Shahroni, C. (2025). Analisis Pengaruh Kuat Tarik Geosintetik Pada Perkuatan Tanah Lunak Metode Geosynthetic Encased Stone Columns (GESC). *Borneo Engineering: Jurnal Teknik Sipil*, *9*(1), 82–93. https://doi.org/10.35334/be.v9i1.32

Herle I., Wehr J., & Arnold M. (2008). Soil improvement with vibrated stone columns: influence of pressure level and relative density on friction angle. *The 2nd International Conference on the Geotechnics of Soft Soils*, 235–240.

Hosseinpour, I., Almeida, M. S. S., & Riccio, M. (2016). Ground improvement of soft soil by geotextile-encased columns. *Proceedings of the Institution of Civil Engineers - Ground Improvement*, *169*(4), 297–305. https://doi.org/10.1680/jgrim.16.00009

Hosseinpour, I., Riccio, M., & Almeida, M. S. S. (2017). Verification of a plane strain model for the analysis of encased granular columns. *Journal of GeoEngineering*, *12*(4), 167–173. https://doi.org/10.6310/jog.2017.12(4).1

Miranda, M., Da Costa, A., Castro, J., & Sagaseta, C. (2015). Influence of gravel density in the behaviour of soft soils improved with stone columns. *Canadian Geotechnical Journal*, *52*(12), 1968–1980. https://doi.org/10.1139/cgj-2014-0487

Murugesan, S., & Rajagopal, K. (2006). Geosynthetic-encased stone columns: Numerical evaluation. *Geotextiles and Geomembranes*, *24*(6), 349–358. https://doi.org/10.1016/j.geotexmem.2006.05.001

Raithel, M., & Kempfert, H. (2000). Calculations models for dam foundations with geotextile coated sand columns. *The International Conference on Geotechnical & Geological Engineering*, 347–352.

Saputra, A., Rokhman, Rini, R. P., Iqbal, & Jafaruddin, A. J. (2025). Peningkatan Nilai Kepadatan Tanah Lunak yang Dicampur dengan Limbah Pasir Galian C dan Air Laut. *Menara: Jurnal Teknik Sipil*, *20*(1), 75–83. https://doi.org/10.21009/jmenara.v20i1.51914